Cancer Imaging (2013) **13(4),** 482–494
DOI: 10.1102/1470-7330.2013.0047

REVIEW

Functional imaging biomarkers for assessing response to treatment in liver and lung metastases

Livia Bernardin, Elizabeth A.M. O'Flynn, Nandita M. deSouza

Clinical Magnetic Resonance Group, Institute of Cancer Research, Royal Marsden NHS Foundation Trust, Downs Road, Sutton, Surrey, UK

Corresponding address: Livia Bernardin, Clinical Magnetic Resonance Group, Institute of Cancer Research, Royal Marsden NHS Foundation Trust, Downs Road, Sutton, Surrey 5M2 5PT, UK.
Email: livia.bernardin@icr.ac.uk, liviabernardin@yahoo.it

Date accepted for publication 24 September 2013

Abstract

Management of patients with metastatic cancer and development of new treatments rely on imaging to provide non-invasive biomarkers of tumour response and progression. The widely used size-based criteria have increasingly become inadequate where early measures of response are required to avoid toxicity of ineffective treatments, as biological, physiologic, and molecular modifications in tumours occur before changes in gross tumour size. A multiparametric approach with the current range of imaging techniques allows functional aspects of tumours to be simultaneously interrogated. Appropriate use of these imaging techniques and their timing in relation to the treatment schedule, particularly in the context of clinical trials, is fundamental. There is a lack of consensus regarding which imaging parameters are most informative for a particular disease site and the best time to image so that, despite an increasing body of literature, open questions on these aspects remain. In addition, standardization of these new parameters is required. This review summarizes the published literature over the last decade on functional and molecular imaging techniques in assessing treatment response in liver and lung metastases.

Keywords: *Liver; lung; metastasis; functional imaging; response; RECIST; volumetry; cell death; metabolism; enhancement.*

Introduction

Ideal oncologic response evaluation criteria should be highly sensitive at an early time point after treatment, as persisting with ineffective treatment increases toxic chemotherapeutic effects, morbidity, and cost[1]. Histopathologic response after treatment correlates best with patient survival and prognosis[2]; however, a direct evaluation of tissue samples before and after treatment is invasive, time consuming, and not always practical[3]. Imaging plays a fundamental role in oncology, providing a non-invasive means of assessing clinical response[4]. However, the widely used anatomic World Health Organization criteria and Response Evaluation Criteria in Solid Tumors (RECIST) 1.0 and 1.1 for the assessment of clinical response to treatment[5–7] are inadequate to assess therapeutic response in early-phase trials of targeted anticancer drugs, as the predominant early effect of therapy requires identification of tumour apoptosis, necrosis, cystic degeneration, and/or intralesional haemorrhage. A reduction in gross tumour size is delayed and lags behind these early biological and molecular modifications[1], so that clinical response criteria defined by size alone can be misleading[8]. During the last decade, significant technical improvements such as very fast multislice computed tomography (CT), cross-sectional three-dimensional multiplanar reconstructions, and whole-body imaging techniques such as positron emission tomography (PET) combined with CT (PET/CT) and diffusion-weighted (DW) magnetic resonance imaging (MRI) have extended the application of imaging in oncology, particularly for therapeutic response assessment in trials of targeted agents[9].

Novel complementary functional and metabolic imaging techniques allow us to explore response at early time points by evaluating alterations in tumour perfusion, oxygenation, and metabolism[10]. The goal of finding a comprehensive set of imaging biomarkers using a multiparametric approach is particularly appealing for therapeutic trials, as it may provide important reliable

indicators of response to new therapies. Biologically validated and reproducible longitudinal functional response assessment of metastases at common sites such as the liver and lung is of major importance in such trials. The QuIConCePT project[11] was set up to biologically validate and establish the reproducibility of 2 key imaging biomarkers: the apparent diffusion coefficient (ADC) and [^{18}F]fluorothymidine (FLT), primarily in liver and lung metastases, to support their future implementation in clinical practice. This review addresses emerging functional and molecular imaging of liver and lung metastatic disease, focusing on practical implications and challenges related to response assessment.

Liver metastases

Several factors favour metastatic seeding within the liver: a high volume of portohepatic blood flow, favourable microscopic sinusoid anatomy that helps trap metastatic cells, and a rich biochemical environment to nourish tumoural cells[12]. Liver metastases are 18–40 times more common than primary liver tumours[13] and are found in 40% of patients dying of cancer[14]. The incidence and pattern of liver metastases are influenced by the patient's age and sex, primary tumour site, histologic type, and length of time since disease onset. Most hepatic metastases are multiple and affect both lobes. A few tumour types, such as colonic carcinoma, carcinoid, and hepatocellular carcinoma (HCC) metastases, may be confined to the liver; however, many other common tumours that metastasize to the liver, such as breast and lung, spread to other sites in the body at the same time. There is a wide published literature on functional measures of response in liver metastases (summarized in Table 1).

Assessing treatment response in liver metastases

Size estimates

Standard RECIST criteria rely on longitudinal two-dimensional measurements of lesions, and do not take into account specific morphologic changes (e.g., tumour necrosis) that frequently occur in response to novel therapeutics. Volumetric estimates are preferred, as they avoid the assumption that tumour grows or shrinks uniformly, although volume extrapolation using one measurement is inaccurate in comparison with that calculated by proper volumetry[15,16]. Volumetric assessment in the liver would eliminate this source of error[16], but it is time consuming, with limited accuracy and reproducibility due to partial volume effects. Measurement errors also occur in small metastatic lesions from using different window settings, slice thickness, and intravenous contrast media[17].

Dynamic enhancement patterns

Antiangiogenic drugs such as bevacizumab, recently introduced into the portfolio for treating colorectal liver metastases, may not necessarily induce changes in tumour size. Morphologic contrast-enhanced CT (CECT) criteria have been shown to be more robust than standard RECIST criteria in predicting response in these instances, because on CECT responding lesions become homogeneously of low attenuation with a smooth, sharp, tumour-normal liver interface. Non-responding lesions lack these changes[18] (Fig. 1).

CT perfusion (CTp)[19], dynamic contrast-enhanced MRI (DCE-MRI), and dynamic contrast-enhanced ultrasound (DCE-US) are a variety of different imaging techniques that offer quantification of various vascular parameters. CTp allows derivation of blood flow (BF), blood volume (BV), capillary permeability (CP), and time to peak enhancement (TTP), which have been used to assess liver metastases of different primary tumours[20,21]. Reduced arterial perfusion was observed after 4–6 weeks treatment with a combination of antiangiogenic drugs for several liver metastases[20]. A reduction in BF and BV was observed less than 48 hours after commencing antiangiogenic treatment in carcinoid liver metastases[21]. CP has been suggested as predictor of response in colorectal liver metastases[22]. The applicability of CTp has increased since the introduction of wider CT detectors and periodic spiral techniques allowing for 15–16-cm craniocaudal coverage with sufficiently short image frequency. Using image registration software can now compensate for respiratory motion. Significant discrepancies between results provided by different commercial software approved for the analyses should be taken into account[23].

DCE-MRI has been mainly used to study colorectal and neuroendocrine liver metastases by extrapolating semi- or fully pharmacokinetic parameters such as area under the concentration curve (AUC), transfer constant K_{trans} (min^{-1}), extracellular extravascular space fractional volume V_e and rate constant k_{ep} (min^{-1}). The optimal mathematical model needed to derive these parameters remains controversial, and different methods are available[24]. An additional quantitative kinetic parameter that can be derived from DCE-MRI is the hepatic perfusion index (HPI). This is the ratio of the hepatic arterial perfusion to the sum of arterial and portal perfusion. Although HPI measurements are potentially more reproducible than K_{trans}[25], changes in the median HPI in liver metastases are observed much later following antiangiogenic treatment. By contrast, a reduction in K_{trans} of up to 47% was detected after 48 h in responders[26,27]. Responding neuroendocrine liver metastases treated with radiolabelled targeted therapy also showed decreased AUC and arterial flow fraction soon after treatment[28]. In addition, both quantitative and semiquantitative parameters correlate with response rate and time to progression of colorectal liver

Table 1 **Literature summary: functional imaging assessing response in liver metastases**

First author, year[Ref.]	No. of patients	Diameter (cm)	Treatment	Timing (D: day, W: week, M: month)	Imaging biomarkers[b]	Results in responders
Ng, 2011[21]	12	≥2	A: Bevacizumab	A: D2, W18	BF, BV, MTT, CP	A: ↓ BV BF
			B: Bevacizumab + IFN	B: D2, W9		B: no measurable IFN effects
	12	≥2	C: IFN × 18 Ws	C: W9, W18	BF, BV, MTT, CP	C: no changes
			D: IFN + bevacizumab	D: D2, W9		D: ↓ BF ↓ BV at D2
Meijerink, 2007[20]	7		AZD2171 + gefitinib	D0, every 4–6 Ws	HAP, HPP	↓ HAP at 1st follow-up
Hirashima, 2012[27]	17	≥1	Bevacizumab + FOLFIRI	D0, W1, every 8 Ws	K_{trans}, K_{ep}	Predictive of response at W1
Morgan, 2003[26]	26	n.a.	Anti-EGF	D0, D2, every 28 Ds	K_i	↓ K_i at D2; ↓ size when ↓ K_i >40%
Miyazaki, 2008[25]	10	≥3	Antiangiogenic	D0, D1, D28	HPI	↓ HPI at D28 (not D1); stable size
Miyazaki, 2012[28]	20	2–9.2	Radiolabelled octreotide	D0, W8	Arterial BV, portal BF, MTT, TDV	↓ TDV and ↑ arterial BF at D0; ↑ TDV at W8
Schrin-Sokhan, 2012[29]	30	n.a.	Bevacizumab	D0, D15, D43	TTP, rise rate	↓ TTP at D0; ↑ TTP on treatment
De Giorgi, 2005[30]	10	n.a.	Imatinib	D0, M6	Not specified	↓ tumour vascularization
Cui, 2008[37]	23	≥1	CHEMO	D0, D3, D7, D42	ADC	↓ ADC at D0; ↑ ADC at D3-D7
Theilmann, 2004[34]	13	≥1	CHEMO	D0, D4, D11, D39	ADC	↑ ADC from D11
Vossen, 2006[35]	n.a.	n.a.	TACE	D0, after TACE	ADC	↑ ADC
	26	5.5	TACE	D0, after TACE	ADC	↑ ADC
Marugami, 2009[38]	11	≥1	HAIC-5FU	D0, D9	ADC_{min}, ADC_{mean}	↑ ADC; ADC_{min} best Sn and Sp
Wybranski, 2011[40]	30	n.a.	High-dose brachytherapy	D0, D2, M3	ADC	↓ ADC at D2; ↑ ADC at M3
Eccles, 2009[42]a	11	n.a.	RT (6 fractions)	D0, W1, W2, M1	ADC	↑ ADC from W1
Dudeck, 2010[41]	21	n.a.	SIRT	D0, D2, W6	ADC	↓ ADC at D2; ↑ ADC and ↓ TV at W6
					Favourable prognosis and outcome	
Lamuraglia, 2006[31]	3	n.a.	Sorafenib	D0, W3, W6	MCU	↓ MCU (↓ or stable tumour volume) at W3
Anzidei, 2011[22]	18	n.a.	CHEMO + antiangiogenetic	D0; M6	BF, BV, CP	↑ CP (NO DIFF in BV BF/ADC variable)
Koh, 2007[36]	20	≥1	CHEMO	D0, W3 from last cycle	ADC	↓ ADCs at D0
Goshen, 2006[45]	7	n.a.	Irinotecan + bevacizumab	D0, cycle 4	SUV	↓ SUV more sensitive to CR than CT
Miller, 2007[50]	27	0.7–16	90Y microsphere SIRT	D0, M1, every 2–3 Ms	SUV	↓ SUV more sensitive to CR than CT

ADC, apparent diffusion coefficient; BF, blood flow; BV, blood volume; CHEMO, standard chemotherapy; CP, capillary permeability; CR, contrast ratio; HAIC-5FU, hepatic arterial infusion chemotherapy + 5-fluorouracil.; HAP, hepatic artery perfusion; HPI, hepatic perfusion index; HPP, hepatic portal perfusion; IFN, interferon; MCU, mean contrast uptake; MTT, mean transit time; SUV, standardized uptake value; TACE, transcatheter arterial chemoembolization; TDV, tumour distribution volume; TTP, time to pick; VEGF, vascular endothelial growth factor.

[a]Includes hepatocellular carcinoma and cholangiocarcinomas.

[b]Derivations of biomarkers: BF, BV, MTT, CP, HAP, HPP (CTp); K_{trans}, k_{ep}, K_i, HPI, BV, BF, MTT, TDV (DCE-MRI); TTP, rise rate, MCU (DCE-US); ADC (DW-MRI); SUV (PET).

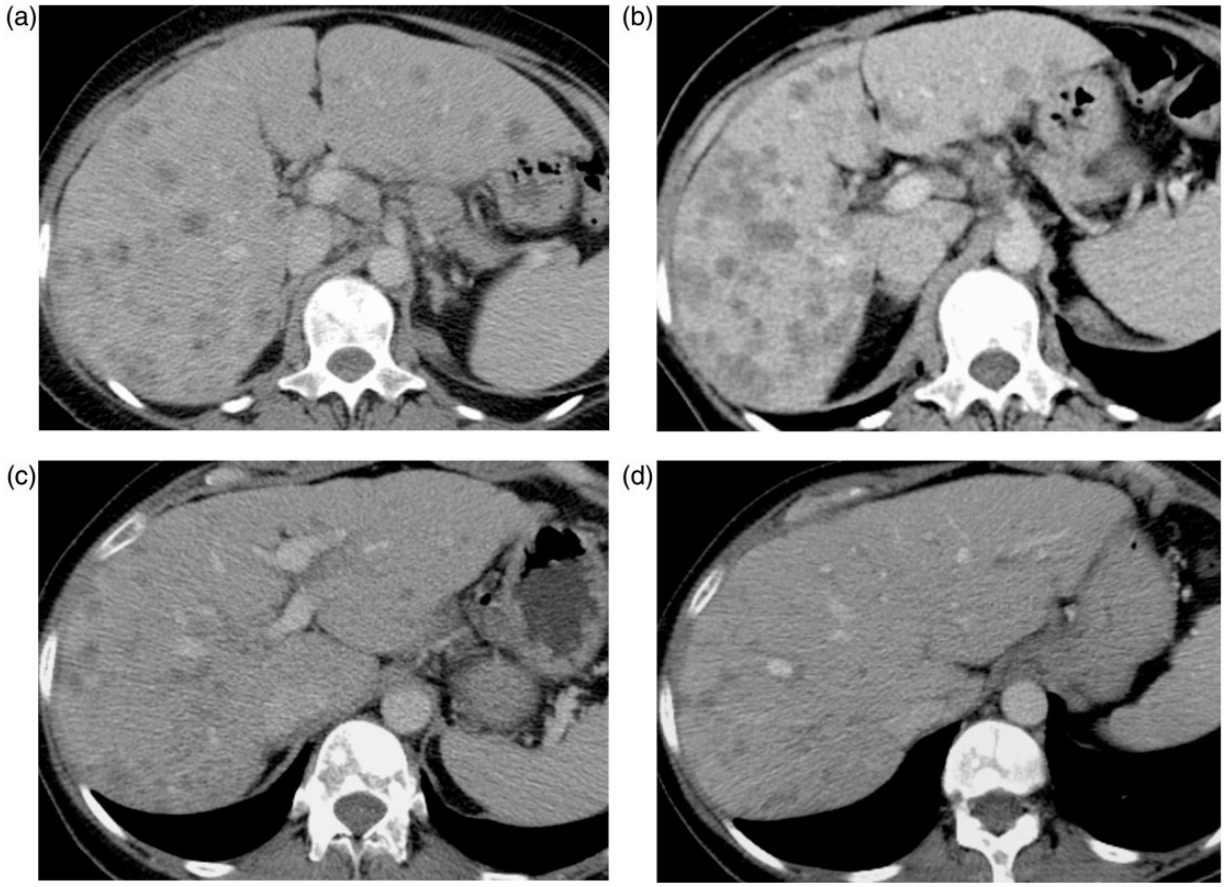

Figure 1 **Metastatic non-small cell lung cancer (NSCLC) on crizotinib. Baseline axial CT (venous phase, A) demonstrates multiple bilobar liver metastases. At 45 days (B), the disease has progressed by size (RECIST) criteria, although lower attenuation of metastases suggests an early response to treatment. Subsequent follow-up images (C, D) at 5 months from baseline confirm a partial response to treatment.**

metastases[27]. The technical limitations of DCE-MRI are mainly related to motion artefacts, which can be reduced by acquiring data in the coronal plane, applying fast breath-hold acquisition techniques, or using respiration-triggered sequences.

The micron-sized gas-filled intravascular microbubble contrast agents used in DCE-US provide a measurement of BV and BF, but not CP. Neovessels as small as 40 μm can be detected with this technique. Parameters such as peak intensity (PI), TTP, AUC, and slope coefficient of enhancement have been evaluated. In metastatic gastrointestinal stromal tumours (GIST), and colorectal and renal cell carcinomas, a strong correlation between the decline of vascular parameters at variable time points (3–43 days) and tumour response was observed before any size reduction[29–31]. Significantly lower baseline TTP values in responders[29] and preliminary results correlating TTP with progression-free survival (PFS) and overall survival (OS) in a metastatic renal carcinoma population[31] illustrate its potential as a predictive imaging biomarker.

To correctly interpret functional imaging modalities that explore vascularity, it is important to remember that tumour heterogeneity is frequently observed at onset and in response to therapy. A reduction in microvascular density of a lesion could coexist with increased tumoural blood perfusion (in case of shunt effects or increased BF through residual viable tumour)[32]. Spatial variation within lesions pre- and posttreatment is also reported with vascular disrupting agents, typically affecting vascularity in the lesion centre but not at the periphery[33].

Estimating cellularity and necrosis

DW-MRI can inform about tumour cellularity and membrane integrity by quantifying the ADC. In responding hepatic metastases significant mean ADC increases have been observed, reflecting a decrease in cell density, an increase in necrosis, and a loss of cell-membrane integrity[34–38] (Fig. 2). Early increases in the ADC at 3–11 days in responding colorectal and breast liver metastases have been found prior to any reduction in size[34,37]. Lower pretreatment mean ADC values may also predict response to chemotherapy in patients with colorectal and

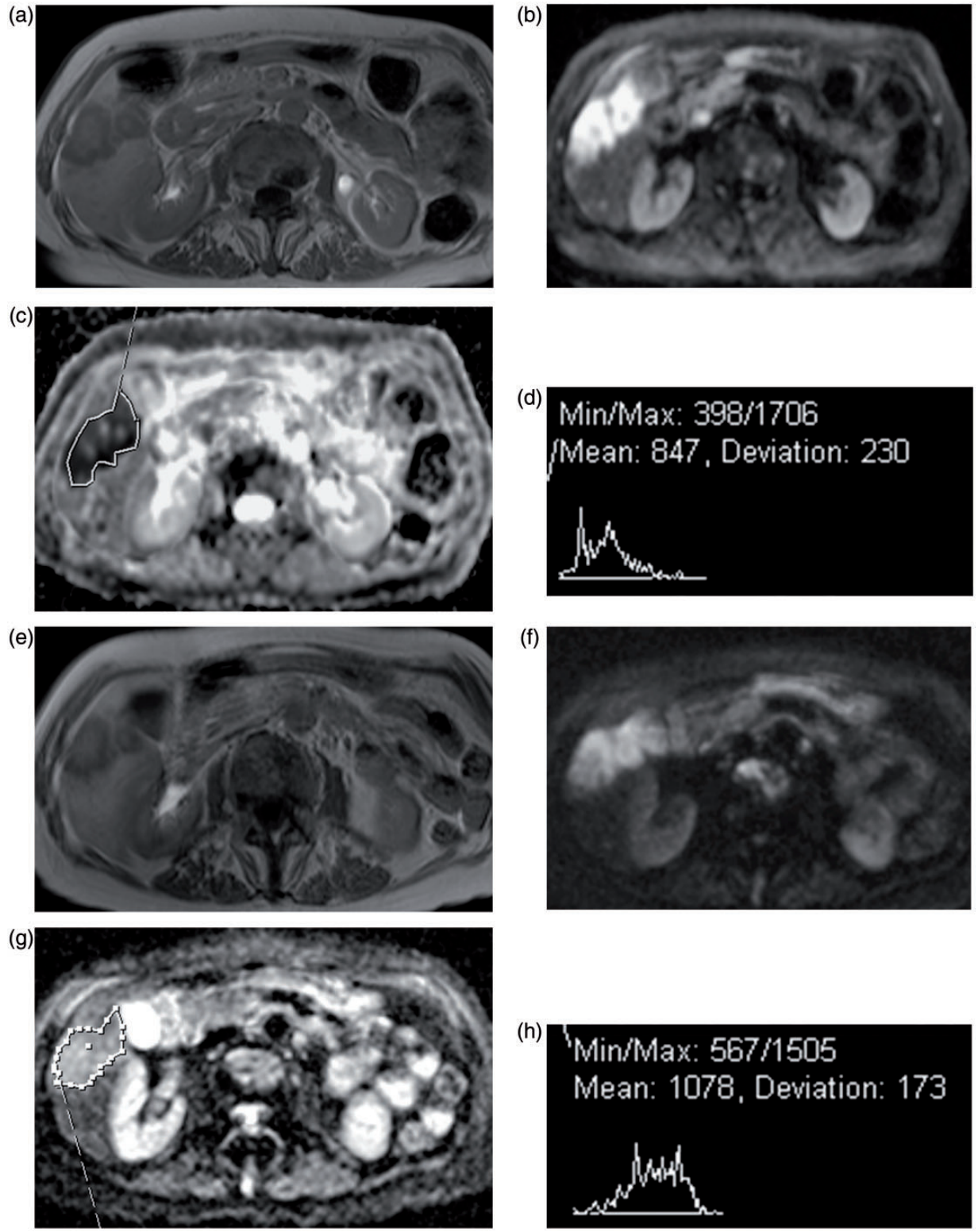

Figure 2 **Metastatic breast cancer treated with lapatinib–capecitabine: axial T1-weighted image 20 minutes after injection of a hepatospecific contrast agent (A), 900 *b* value DWI (B), and corresponding ADC map (C) before treatment. Metastatic deposits in segment V/VI of the liver show restricted diffusion (ADC value = 0.85×10^{-3}/mm^2/s). After 3 months of treatment, no significant change in size is demonstrated on the delayed postcontrast T1-weighted image (E), whereas the ADC value has increased to 1.08×10^{-3}/mm^2/s as demonstrated qualitatively (F, G) and by histogram analysis before and after treatment, respectively (D, H), suggesting a response to treatment.**

gastric hepatic metastases[39]. A weak, but significant, correlation between final tumour size, lower pretreatment ADC value, and early increase in ADC has also been reported[37].

In patients responding to radiation therapy, brachytherapy pellets and selective internal radiotherapy (SIRT) can cause a temporary, paradoxical drop in the ADC 2 days after commencing treatment with an associated early increase in tumour volume. This is then followed by an eventual increase in the ADC and lesion shrinkage at 3 months[40,41], thought to be a consequence of early transient cell swelling and transudation of plasma components into the extravascular extracellular space[40,41]. Radiation effects on tissues vary depending on dose and number of fractions delivered, but overall there is a larger increase in ADC seen in responders in comparison with non-responders[42].

Metabolic effects

[^{18}F]Fluorodeoxyglucose (FDG)-PET is reported to have sensitivity of 100% and specificity of 90% in predicting response to chemotherapy in colorectal liver metastases after 4–5 weeks[43], with treatment effects detected much earlier than if standard RECIST criteria are used (4 weeks versus 2–4 months)[44]. False-positive results from inflammation are seen, however, and not every tumour is hypermetabolic, meaning baseline maximum standardized uptake values (SUV_{max}) are critical. The absence of residual metabolic activity after treatment, even in lesions that have not significantly reduced in size, is proposed as a response biomarker[45]. However, a recent case–control study indicates a high false-negative rate at a 4-week time point, likely attributable to metabolic inhibition caused by chemotherapy agents[46]. Furthermore, complete metabolic response after neoadjuvant chemotherapy for colorectal liver metastases was reported to be an unreliable indicator of complete pathologic response, with microscopic viable tumour still present on histopathologic examination in the majority of metabolically inactive lesions[47]. One study reported that FDG-PET changes after 2 months of chemotherapy was able to predict long-term survival[48], although these results have not been corroborated[46]. Combining morphologic features suggestive of necrosis on CT with size criteria and FDG-PET may also significantly improve the accuracy of response assessment for radionuclide (yttrium-90 microsphere) treatment[49,50].

FLT is an alternative radiotracer for imaging cell proliferation. Although FLT-PET correlates with the cellular proliferation marker (Ki-67) in metastatic colorectal cancer[51], the high physiologic uptake of FLT limits its

Table 2 **Literature summary: functional imaging for NSCLC and lung metastases[a]**

First author, year[Ref.]	No. of patients	Diameter (cm)	Treatment	Timing (H: hours, D: day, W: week, M: month)	Imaging biomarkers[b]	Results in responders
Harvey, 2002[64]	3	n.a.	FRT	D0, W1, W2, W6, W12	Perfusion, CP	↑ perfusion, ↑ CP at W1–W2
Wang, 2009[63]	35	≥3	CHEMO (19) RT (7) CHEMORT (9)	D0, cycle2, end RT	BV, BF, CP, MTT	↑ BF at D0 ↓ BV, BF, CP post RT ± CHEMO (no changes with chemo only)
Ng, 2007[66]	16	4.9–11.8	FRT	D0, 2–4-6 fractions	BV, CP	↑ BV at fraction 2–4 (not 6)
Ng, 2007[65]	8	4.9–11.8	RT + VDA	D0,2 fractions H4, H72 post VDA	BV, CP	↑ BV, ↑ CP at fraction 2 ↓ BV at H4–H72
Hegenscheid, 2010[68]a	22	0.8–5.4	LITT	D0, D1, W4, W6	BV, BF, CP, MTT	↓ BV, BF, CP at D1, W4, W6 Correlation with RECIST at M12
Yabuuchi, 2011[67]	28	2.3–9	CHEMO	D0, W3,W4	TTP, WashOut MaxEnh ratio	No change at W3,W4
					ADC	↑ ADC at W3, W4 (↓ size at W6, W8)
Chang, 2012[74]	14	≥3	CHEMORT	D0, at 40Gy	ADC	↑ ADC at 40 Gy
Okuma, 2009[73]a	20	1–4.5	RFA	D0, D3	ADC	↑ ADC at D3
Lee, 2009[77]	31	n.a.	CHEMO	D0, W3	SUV_{max}	↓ SUV
MacManus, 2003[78]	10	n.a.	RT	D0, W, W12	Qualitative assessment	↓ visual uptake
	61		CHEMORT		Favourable prognosis and outcome	
Ohno, 2012[72]	64	≥1	CHEMORT	D0	ADC	↓ ADC superior to ↓ SUV_{max} to predict response
					SUV_{max}	
de Geus-Oei, 2007[79]	51	n.a.	CHEMO	D0, W5,W8	SUV	↓ SUV is prognostic

ADC, apparent diffusion coefficient; BF, blood flow; BV, blood volume; CHEMO, chemotherapy; CHEMORT, chemoradiotherapy; CP, capillary permeability; FRT, fractionated radiotherapy; Gy, gray; LITT, laser-induced thermal therapy; ls, lesions; Max Enh, maximum enhancement; MTT, mean transit time; NSCLC, non-small cell lung cancer; RFA, radiofrequency ablation.; RT, radiotherapy; SUV, standardized uptake value; TTP, time to peak; VDA, vascular disruptive agent.

[a]Includes lung metastases.

[b]Derivations of biomarkers: perfusion, BV, BF, CP, MTT (CTp); TTP, WashOut, Max Enh ratio (DCE-MRI); ADC (DW-MRI); SUV, SUV_{max} (PET).

utility in assessing the liver. Using a kinetic filtering method that highlights liver metastatic uptake and excludes normal liver background uptake, a significant reduction in FLT was found in responders 2 weeks after treatment[52].

In vivo magnetic resonance spectroscopy (MRS) of the liver is a potential alternative method for quantifying metabolic and biochemical composition of lesions. In contrast to FDG-PET/CT, MRS of the liver is particularly challenging because of respiratory motion, poor signal to noise ratio (SNR), magnetic field inhomogeneity, and contamination from out-of-voxel signals. Although proton (^{1}H), phosphorus (^{31}P), and carbon-13 (^{13}C) MRS is possible, hydrogen is the most studied nucleus because of its best reported sensitivity. A significant reduction of the choline spectral peak after transcatheter arterial chemoembolization has been shown in HCC[53], but no similar data are available for liver metastases.

Lung metastases

Pulmonary metastases are common, as the entire cardiac output flows through the lungs. Most frequently they occur with breast, colorectal, bronchial, bladder, renal, and head and neck cancers. Pulmonary metastases are found in up to 54% of patients dying of cancer, but their incidence at presentation is lower and varies depending on the primary tumour[54]. Pulmonary metastases are usually multiple; solitary metastases are uncommon and most likely from colorectal cancer. Morphologic features can correlate with the primary site of disease, with miliary micronodular dissemination indicating melanoma and thyroid cancer, large lobulated masses sarcomas, cavitating lesions squamous cell carcinomas, calcifications osteosarcomas and infiltrative or pneumonia-like pattern adenocarcinomas[55]. In all cases, the presence of lung metastases is a poor prognostic factor.

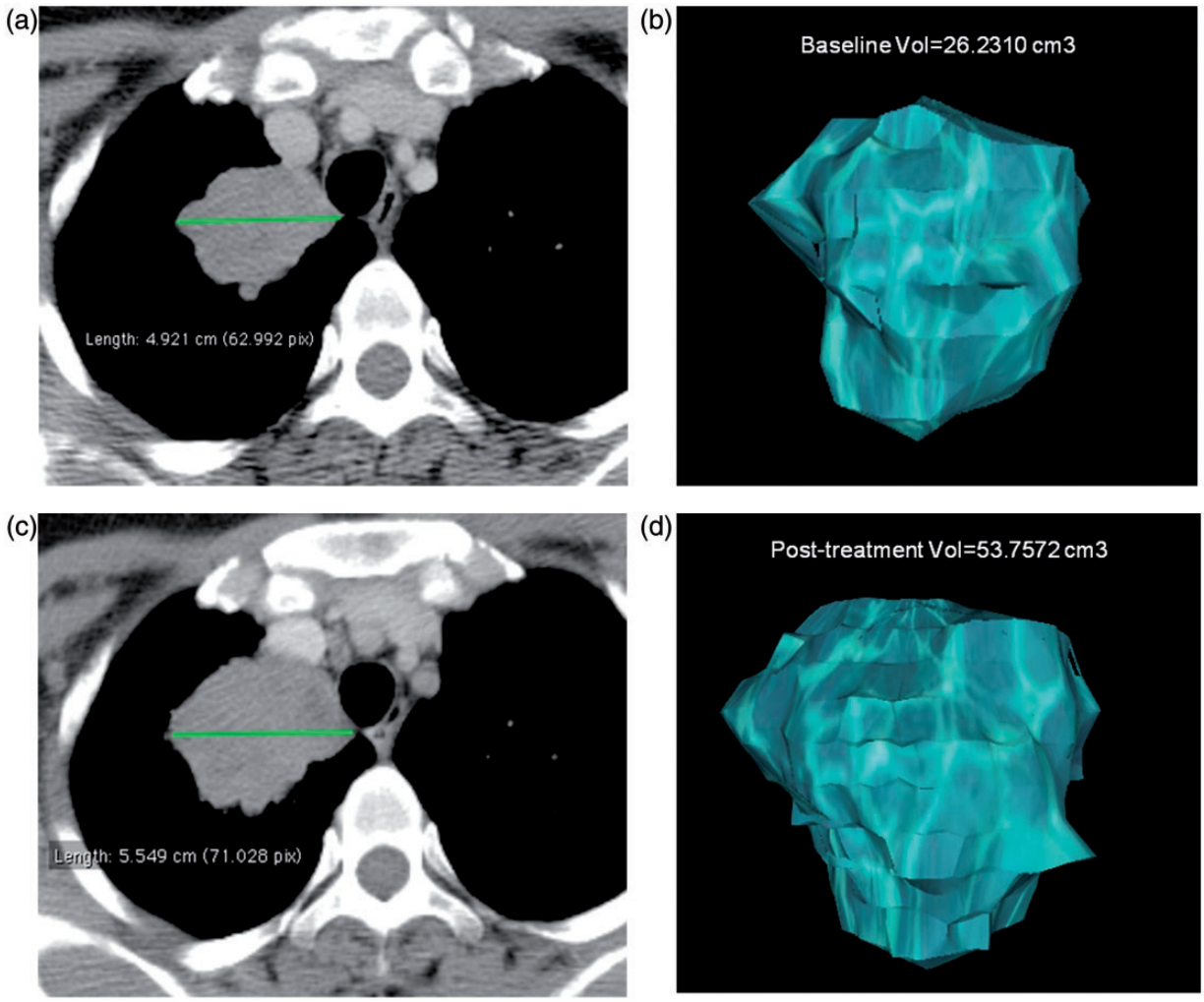

Figure 3 **Volumetric assessment of lung metastasis. CT (A) and segmented volume (B) in a right upper lobe target lesion with corresponding images (C, D) after 2 cycles of carboplatin. Although the disease is stable by RECIST criteria (<20% increase of the maximum diameter in the interval), the volumetric assessment of the same target lesion indicates that the lesion has doubled in volume (B vs D) in the interval, suggesting disease progression.**

Imaging the lungs poses unique challenges attributable to intrinsic respiratory motion and air content, which particularly affects MRI as there is low proton density and fast signal decay. In addition, significant tumoural and interpatient heterogeneity is reported, with divergent treatment responses[56,57]. Only 2 studies report response to functional imaging parameters in lung metastases, and more data are available for primary tumours (Table 2).

Assessing treatment response in lung lesions

Size estimates

RECIST criteria are limited in the assessment of lung nodules, as most of them do not grow uniformly and target lesions do not necessarily represent the gross pulmonary disease burden[58]. Surrounding inflammation and atelectasis also obscure tumour foci on morphologic imaging alone. Nodules adjacent to the pleura and situations where neighbouring vessels are not distinguished from tumour make accurate lesion location challenging[59]. Automatic segmentation methods are more reproducible and accurate (reported accuracy within 3% for 3-mm nodules) than one- or two-dimensional measurements, and decrease interobserver variation in RECIST measurements[60].

Arbitrary selection of lesions as targets could significantly influence therapeutic response perception. A study including only 35% of the total number of lung nodules resulted in a different response assignment when compared with assessment of 100% of lung nodules[57]. Interobserver agreement varied significantly when the number of targets was changed from 5 to 1, suggesting that at least 3 lesions should be followed up during treatment[61]. A volume change of 30–40%[62] has recently been proposed to differentiate stable from progressive disease, but is not currently standard practice (Fig. 3).

Dynamic enhancement patterns

Quantified vascular parameters such as BF, BV, mean transit time (MTT), and CP are starting to be exploited for the assessment of response of lung lesions[63–68] in therapeutic trials. CTp parameters and microvascular density correlate with vascular endothelial growth factor, and are of potential value in monitoring antivascular treatments[69]. In non-small cell lung cancer (NSCLC) tumours, baseline BF was significantly higher

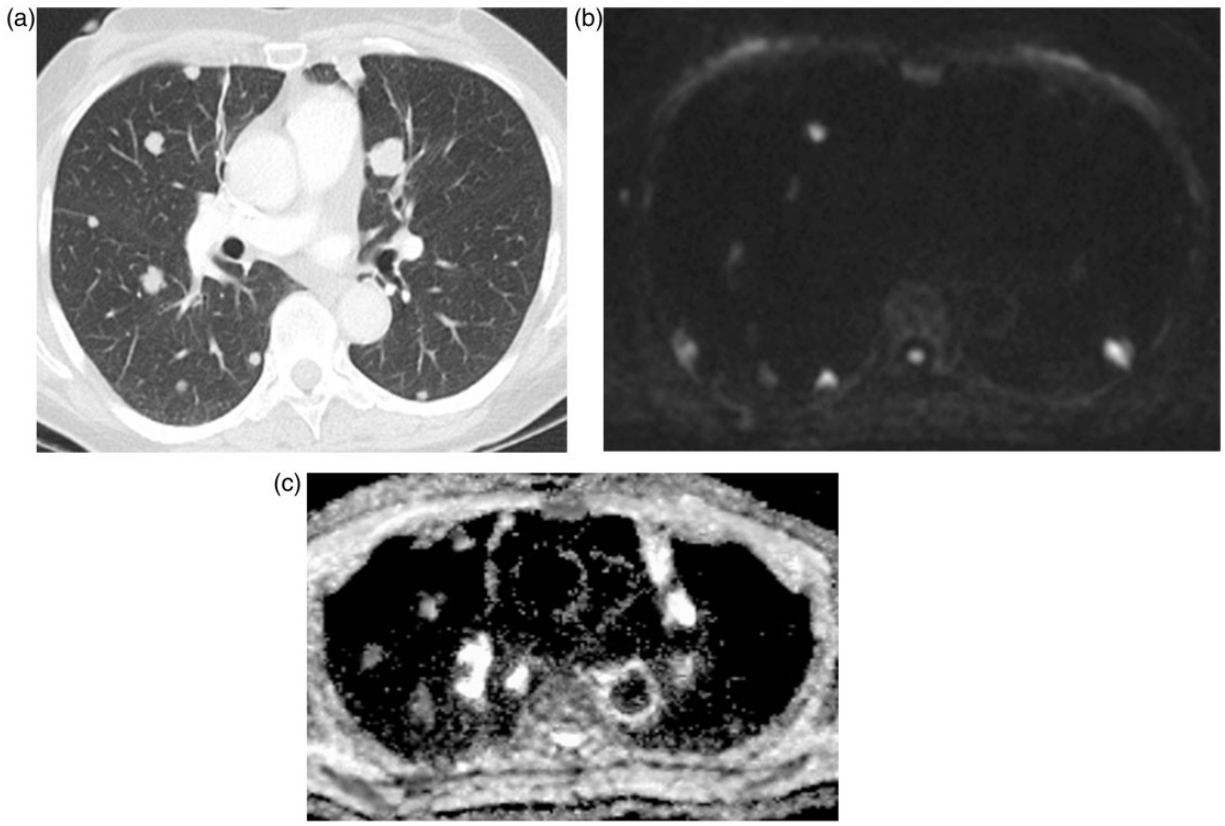

Figure 4 **DW-MRI in lung metastases. Axial CT image shows multiple small bilateral lung metastases (≤13 mm) (A). These lesions are identified on a high *b* value DW image (*b*800, B) and have a low ADC value (0.4–0.7 × 10^{-3}/mm^2/s) compared with muscle (1.3 × 10^{-3}/mm^2/s) on the ADC map (C).**

in responders than in non-responders after radiotherapy or combined chemoradiotherapy, with a significant decrease in BF, BV, and CP, and an increase in MTT after treatment[63]; these differences were not seen with chemotherapy alone. CTp can assess whole lung tumours with a reproducibility of 10% for BV and 30% for tumour permeability[70]. Issues related to the long breath-hold required (approximately 40 s) have been overcome with technical development and implementation of image registration algorithms to correct misregistration.

Very little is known regarding the use of DCE-MRI to assess response to treatment of lung primaries, and there are no dedicated data for lung metastases. Lung DCE-MRI protocols and analysis methods vary considerably, and modelling pulmonary tumour enhancement is complex in the context of dual blood circulation and positional BF variation. In 28 patients with NSCLC, no significant differences between baseline and postchemotherapy (1 cycle) vascular parameters such as time to peak, washout ratio, and maximum enhancement ratio were achieved following variable treatment with cytotoxic and cytostatic agents[67].

Estimating cellularity and necrosis

DW-MRI of the lung is gaining interest (Figs. 4 and 5) for monitoring treatment response of lung lesions[71]; however, there are no data dedicated specifically to lung metastases. Baseline ADC values in NSCLC are predictive of chemoradiotherapy and radiofrequency ablation response[72,73] with pretreatment ADCs $\leq 2 \times 10^{-3}\,mm^2/s$ indicating longer PFS. ADC values have been shown to increase in response to chemoradiation, with mean percentage increase much higher than percentage decrease in tumour diameter[67,74]. Changes in the ADC may be more effective than DCE-MRI in these studies, probably because antiangiogenetic agents were not part of the treatment regimens. However, there are no consensus protocols for lung DW-MRI, and the reproducibility of ADC measurements in the lung needs to be established.

Metabolic effects

The poor spatial resolution of PET has been partly resolved by integrated PET/CT imaging. Dedicated

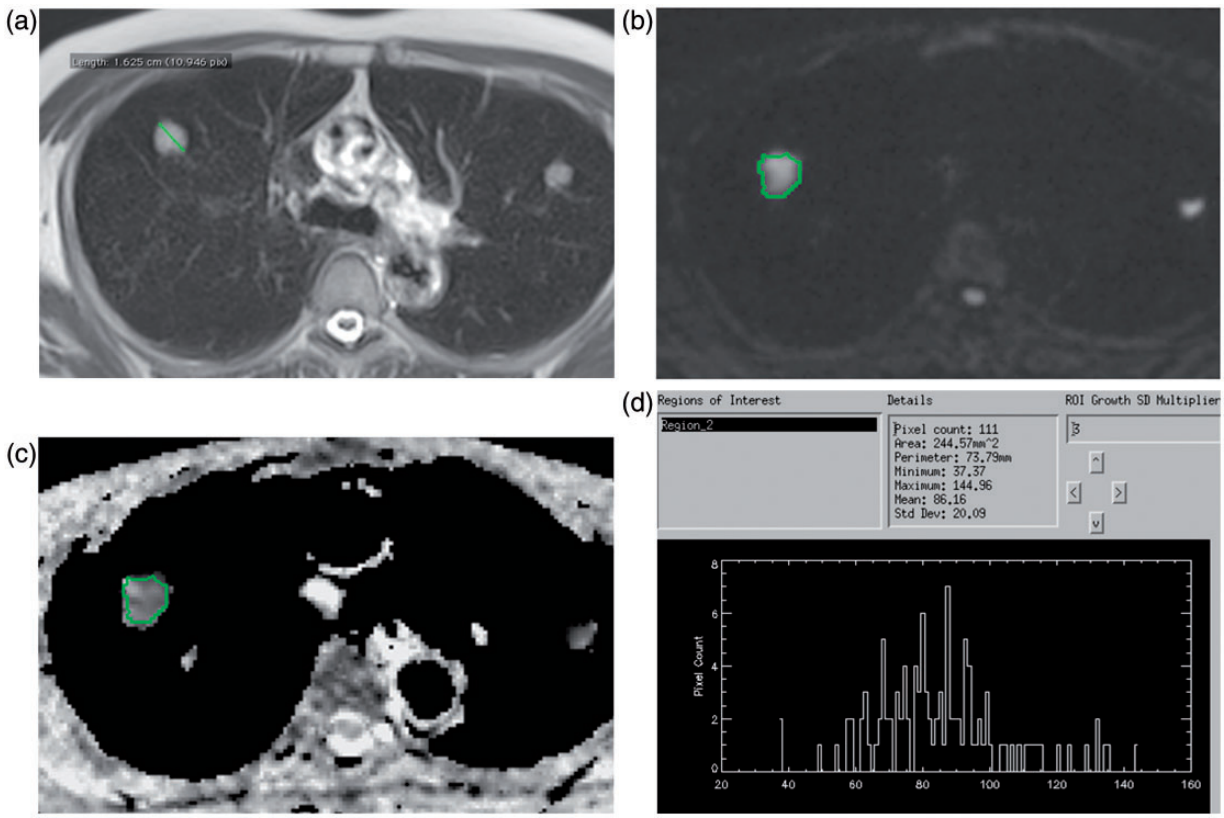

Figure 5 **Quantification of ADC in lung metastases. Axial T2 HASTE image (A), DWI (*b*800, B), and ADC map (C) showing a dominant 16-mm right lung metastasis. Pixel-by-pixel quantification of the ADC is performed by drawing a region of interest (ROI) around the lesion and determining the rate of decay of signal using a monoexponential fit of the data (ADEPT in-house software; ICR, UK). A minimum, maximum, and mean value of ADC can be derived for the ROI as well as a histogram plot of the ADC distribution in the lesion (D).**

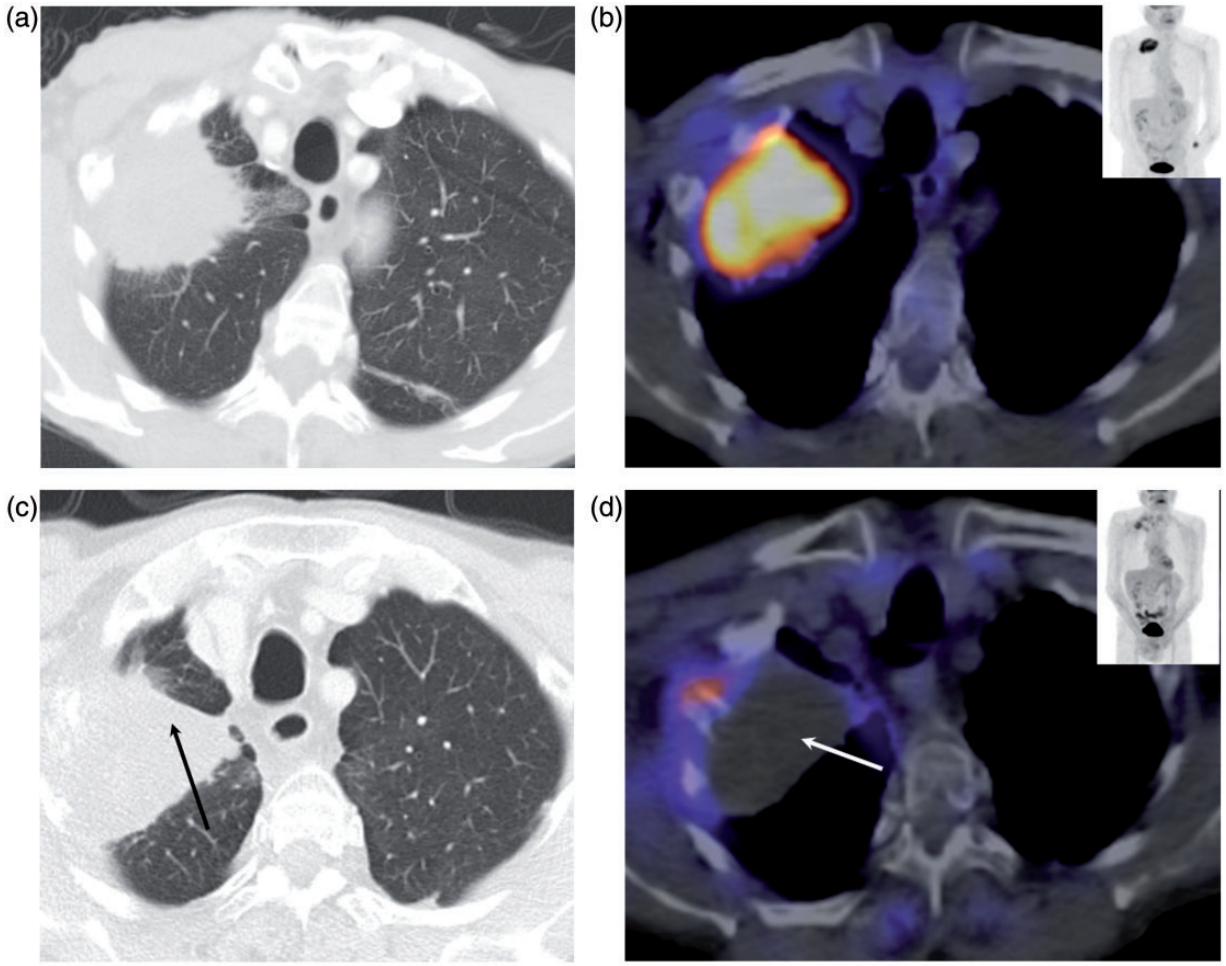

Figure 6 **Metabolic response assessment of lung metastasis on FDG-PET/CT. CT (A) and fused FDG-PET/CT (B) in NSCLC before treatment with corresponding images (C and D) post treatment showing that concomitant atelectasis makes it difficult to assess response to treatment on CT alone (black arrow, C). Following treatment there is almost complete metabolic activity shutdown within the lesion (white arrow, D) indicating treatment response.**

studies assessing response in lung metastases using PET or PET/CT are not available, although primary NSCLCs have been investigated by several authors[75–79]. Metabolic response after 1–3 cycles of chemotherapy is a better prognostic factor than size estimate on CT (Fig. 6), and correlated well with the final outcome of treatment[79]. There are inconsistent reports on the influence of metabolic response on long-term outcome, with one group suggesting that an early metabolic response does not translate into better survival outcome,[77] whereas another reported a significantly longer median survival for patients with complete early metabolic response[78,79].

Conclusion

Accurate measurement of metastatic tumour burden using imaging, both pretreatment and posttreatment, is crucial for assessing response within clinical trials. Over and above measures of disease burden, imaging can inform about the effects of treatment on tissues at early time points by selecting the most appropriate multiparametric imaging biomarkers and timing for their measurement on the basis of specific effects on tumour biology. However, technical challenges of making robust and reproducible measurements in a multicenter setting mean that there is a paucity of data using functional imaging studies, particularly in the assessment of metastatic lung disease. Imaging standardization within the EU/Pharma-funded QuiConCePT project should provide a platform to support and guide the future development and implementation of imaging biomarkers in multicenter response-assessment trials.

Acknowledgements

We acknowledge the support received from the Innovative Medicine Initiative (IMI) European Union

funding to QuIC-ConCePT, grant EEC100X. We would also like to acknowledge James d'Arcy and the ICR for providing the in-house ADEPT software for DW-MRI analysis. Supported by Innovative Medicine Initiative (IMI) European Union funding to QuIC-ConCePT, grant EEC100X.

Conflict of interest

L.B., related financial activities: EEC100X grant from IMI EU funding to QuIConCePT. E.O'F., none; N.deS, none.

References

[1] Harry VN, Semple SI, Parkin DE, Gilbert FJ. Use of new imaging techniques to predict tumour response to therapy. Lancet Oncol 2010; 11: 92–102.
[2] Serkova NJ, Garg K, Bradshaw-Pierce EL. Oncologic imaging end-points for the assessment of therapy response. Recent Pat Anticancer Drug Discov 2009; 4: 36–53.
[3] Sullivan DC, Gatsonis C. Response to treatment series: part 1 and introduction, measuring tumor response–challenges in the era of molecular medicine. AJR Am J Roentgenol 2011; 197: 15–17.
[4] Jaffe CC. Measures of response: RECIST, WHO, and new alternatives. J Clin Oncol 2006; 24: 3245–3251.
[5] Palmer DB. WHO handbook for reporting results of cancer treatment. Br J Cancer 1982; 45: 484–485.
[6] Therasse P, Arbuck SG, Eisenhauer EA, et al. New guidelines to evaluate the response to treatment in solid tumors. European Organization for Research and Treatment of Cancer, National Cancer Institute of the United States, National Cancer Institute of Canada. J Natl Cancer Inst 2000; 92: 205–216.
[7] Eisenhauer EA, Therasse P, Bogaerts J, et al. New response evaluation criteria in solid tumours: revised RECIST guideline (version 1.1). Eur J Cancer 2009; 45: 228–247.
[8] Van Beers BE, Vilgrain V. Biomarkers in abdominal imaging. Abdom Imaging 2009; 34: 663–667.
[9] Gwyther SJ, Schwartz LH. How to assess anti-tumour efficacy by imaging techniques. Eur J Cancer 2008; 44: 39–45.
[10] Marcus CD, Ladam-Marcus V, Cucu C, Bouche O, Lucas L, Hoeffel C. Imaging techniques to evaluate the response to treatment in oncology: current standards and perspectives. Crit Rev Oncol Hematol 2009; 72: 217–238.
[11] QuIC-ConCePT. Quantitative imaging in cancer: connecting cellular processes with therapy. Available from: http://www.quic-concept.eu/.
[12] Robinson PJ. Imaging liver metastases: current limitations and future prospects. Br J Radiol 2000; 73: 234–241.
[13] Imam K, Bluemke DA. MR imaging in the evaluation of hepatic metastases. Magn Reson Imaging Clin North Am 2000; 8: 741–756.
[14] Beckingham IJ, Krige JE. ABC of diseases of liver, pancreas, and biliary system. BMJ 2001; 322: 477–480.
[15] Mantatzis M, Kakolyris S, Amarantidis K, Karayiannakis A, Prassopoulos P. Treatment response classification of liver metastatic disease evaluated on imaging. Are RECIST unidimensional measurements accurate? Eur Radiol 2009; 19: 1809–1816.
[16] Prasad SR, Jhaveri KS, Saini S, Hahn PF, Halpern EF, Sumner JE. CT tumor measurement for therapeutic response assessment: comparison of unidimensional, bidimensional, and volumetric techniques initial observations. Radiology 2002; 225: 416–419.
[17] Sohaib SA, Turner B, Hanson JA, Farquharson M, Oliver RT, Reznek RH. CT assessment of tumour response to treatment: comparison of linear, cross-sectional and volumetric measures of tumour size. Br J Radiol 2000; 73: 1178–1184.
[18] Boonsirikamchai P, Asran MA, Maru DM, et al. CT findings of response and recurrence, independent of change in tumor size, in colorectal liver metastasis treated with bevacizumab. AJR Am J Roentgenol 2011; 197: W1060–W1066.
[19] Goetti R, Leschka S, Desbiolles L, et al. Quantitative computed tomography liver perfusion imaging using dynamic spiral scanning with variable pitch: feasibility and initial results in patients with cancer metastases. Invest Radiol 2010; 45: 419–426.
[20] Meijerink MR, van Cruijsen H, Hoekman K, et al. The use of perfusion CT for the evaluation of therapy combining AZD2171 with gefitinib in cancer patients. Eur Radiol 2007; 17: 1700–1713.
[21] Ng CS, Charnsangavej C, Wei W, Yao JC. Perfusion CT findings in patients with metastatic carcinoid tumors undergoing bevacizumab and interferon therapy. AJR Am J Roentgenol 2011; 196: 569–576.
[22] Anzidei M, Napoli A, Zaccagna F, et al. Liver metastases from colorectal cancer treated with conventional and antiangiogenetic chemotherapy: evaluation with liver computed tomography perfusion and magnetic resonance diffusion-weighted imaging. J Comput Assist Tomogr 2011; 35: 690–696.
[23] Miles KA. Functional computed tomography in oncology. Eur J Cancer 2002; 38: 2079–2084.
[24] O'Connor JP, Tofts PS, Miles KA, Parkes LM, Thompson G, Jackson A. Dynamic contrast-enhanced imaging techniques: CT and MRI. Br J Radiol 2011; 84(Spec No 2): S112–120.
[25] Miyazaki K, Collins DJ, Walker-Samuel S, et al. Quantitative mapping of hepatic perfusion index using MR imaging: a potential reproducible tool for assessing tumour response to treatment with the antiangiogenic compound BIBF 1120, a potent triple angiokinase inhibitor. Eur Radiol 2008; 18: 1414–1421.
[26] Morgan B, Thomas AL, Drevs J, et al. Dynamic contrast-enhanced magnetic resonance imaging as a biomarker for the pharmacological response of PTK787/ZK 222584, an inhibitor of the vascular endothelial growth factor receptor tyrosine kinases, in patients with advanced colorectal cancer and liver metastases: results from two phase I studies. J Clin Oncol 2003; 21: 3955–3964.
[27] Hirashima Y, Yamada Y, Tateishi U, et al. Pharmacokinetic parameters from 3-Tesla DCE-MRI as surrogate biomarkers of antitumor effects of bevacizumab plus FOLFIRI in colorectal cancer with liver metastasis. Int J Cancer 2012; 130: 2359–2365.
[28] Miyazaki K, Orton MR, Davidson RL, et al. Neuroendocrine tumor liver metastases: use of dynamic contrast-enhanced MR imaging to monitor and predict radiolabeled octreotide therapy response. Radiology 2012; 263: 139–148.
[29] Schirin-Sokhan R, Winograd R, Roderburg C, et al. Response evaluation of chemotherapy in metastatic colorectal cancer by contrast enhanced ultrasound. World J Gastroenterol 2012; 18: 541–545.
[30] De Giorgi U, Aliberti C, Benea G, Conti M, Marangolo M. Effect of angiosonography to monitor response during imatinib treatment in patients with metastatic gastrointestinal stromal tumors. Clin Cancer Res 2005; 11: 6171–6176.
[31] Lamuraglia M, Escudier B, Chami L, et al. To predict progression-free survival and overall survival in metastatic renal cancer treated with sorafenib: pilot study using dynamic contrast-enhanced Doppler ultrasound. Eur J Cancer 2006; 42: 2472–2479.
[32] Kan Z, Phongkitkarun S, Kobayashi S, et al. Functional CT for quantifying tumor perfusion in antiangiogenic therapy in a rat model. Radiology 2005; 237: 151–158.
[33] Gaya AM, Rustin GJ. Vascular disrupting agents: a new class of drug in cancer therapy. Clin Oncol (R Coll Radiol) 2005; 17: 277–290.
[34] Theilmann RJ, Borders R, Trouard TP, et al. Changes in water mobility measured by diffusion MRI predict response of metastatic breast cancer to chemotherapy. Neoplasia 2004; 6: 831–837.

[35] Vossen JA, Buijs M, Kamel IR. Assessment of tumor response on MR imaging after locoregional therapy. Tech Vasc Interv Radiol 2006; 9: 125–132.

[36] Koh DM, Collins DJ. Diffusion-weighted MRI in the body: applications and challenges in oncology. AJR Am J Roentgenol 2007; 188: 1622–1635.

[37] Cui Y, Zhang XP, Sun YS, Tang L, Shen L. Apparent diffusion coefficient: potential imaging biomarker for prediction and early detection of response to chemotherapy in hepatic metastases. Radiology 2008; 248: 894–900.

[38] Marugami N, Tanaka T, Kitano S, et al. Early detection of therapeutic response to hepatic arterial infusion chemotherapy of liver metastases from colorectal cancer using diffusion-weighted MR imaging. Cardiovasc Intervent Radiol 2009; 32: 638–646.

[39] Koh DM, Scurr E, Collins D, et al. Predicting response of colorectal hepatic metastasis: value of pretreatment apparent diffusion coefficients. AJR Am J Roentgenol 2007; 188: 1001–1008.

[40] Wybranski C, Zeile M, Lowenthal D, et al. Value of diffusion weighted MR imaging as an early surrogate parameter for evaluation of tumor response to high-dose-rate brachytherapy of colorectal liver metastases. Radiat Oncol 2011; 6: 43.

[41] Dudeck O, Zeile M, Wybranski C, et al. Early prediction of anticancer effects with diffusion-weighted MR imaging in patients with colorectal liver metastases following selective internal radiotherapy. Eur Radiol 2010; 20: 2699–2706.

[42] Eccles CL, Haider EA, Haider MA, Fung S, Lockwood G, Dawson LA. Change in diffusion weighted MRI during liver cancer radiotherapy: preliminary observations. Acta Oncol 2009; 48: 1034–1043.

[43] Findlay M, Young H, Cunningham D, et al. Noninvasive monitoring of tumor metabolism using fluorodeoxyglucose and positron emission tomography in colorectal cancer liver metastases: correlation with tumor response to fluorouracil. J Clin Oncol 1996; 14: 700–708.

[44] Bystrom P, Berglund A, Garske U, et al. Early prediction of response to first-line chemotherapy by sequential [^{18}F]-2-fluoro-2-deoxy-D-glucose positron emission tomography in patients with advanced colorectal cancer. Ann Oncol 2009; 20: 1057–1061.

[45] Goshen E, Davidson T, Zwas ST, Aderka D. PET/CT in the evaluation of response to treatment of liver metastases from colorectal cancer with bevacizumab and irinotecan. Technol Cancer Res Treat 2006; 5: 37–43.

[46] Glazer ES, Beaty K, Abdalla EK, Vauthey JN, Curley SA. Effectiveness of positron emission tomography for predicting chemotherapy response in colorectal cancer liver metastases. Arch Surg 2010; 145: 340–345; discussion 345.

[47] Tan MC, Linehan DC, Hawkins WG, Siegel BA, Strasberg SM. Chemotherapy-induced normalization of FDG uptake by colorectal liver metastases does not usually indicate complete pathologic response. J Gastrointest Surg 2007; 11: 1112–1119.

[48] de Geus-Oei LF, van Laarhoven HW, Visser EP, et al. Chemotherapy response evaluation with FDG-PET in patients with colorectal cancer. Ann Oncol 2008; 19: 348–352.

[49] Lewandowski RJ, Thurston KG, Goin JE, et al. 90Y microsphere (TheraSphere) treatment for unresectable colorectal cancer metastases of the liver: response to treatment at targeted doses of 135–150 Gy as measured by [^{18}F]fluorodeoxyglucose positron emission tomography and computed tomographic imaging. J Vasc Interv Radiol 2005; 16: 1641–1651.

[50] Miller FH, Keppke AL, Reddy D, et al. Response of liver metastases after treatment with yttrium-90 microspheres: role of size, necrosis, and PET. AJR Am J Roentgenol 2007; 188: 776–783.

[51] Francis DL, Freeman A, Visvikis D, et al. In vivo imaging of cellular proliferation in colorectal cancer using positron emission tomography. Gut 2003; 52: 1602–1606.

[52] Contractor K, Challapalli A, Tomasi G, et al. Imaging of cellular proliferation in liver metastasis by [(18)F]fluorothymidine positron emission tomography: effect of therapy. Phys Med Biol 2012; 57: 3419–3433.

[53] Kuo YT, Li CW, Chen CY, Jao J, Wu DK, Liu GC. In vivo proton magnetic resonance spectroscopy of large focal hepatic lesions and metabolite change of hepatocellular carcinoma before and after transcatheter arterial chemoembolization using 3.0-T MR scanner. J Magn Reson Imaging 2004; 19: 598–604.

[54] Crow J, Slavin G, Kreel L. Pulmonary metastasis: a pathologic and radiologic study. Cancer 1981; 47: 2595–2602.

[55] Akira W, editor. Cancer metastases research. Nova Science Publishers; 2008.

[56] Chojniak R, Younes RN. Pulmonary metastases tumor doubling time: assessment by computed tomography. Am J Clin Oncol 2003; 26: 374–377.

[57] Chojniak R, Yu LS, Younes RN. Response to chemotherapy in patients with lung metastases: how many nodules should be measured? Cancer Imaging 2006; 6: 107–112.

[58] Tran LN, Brown MS, Goldin JG, et al. Comparison of treatment response classifications between unidimensional, bidimensional, and volumetric measurements of metastatic lung lesions on chest computed tomography. Acad Radiol 2004; 11: 1355–1360.

[59] Bogot NR, Kazerooni EA, Kelly AM, Quint LE, Desjardins B, Nan B. Interobserver and intraobserver variability in the assessment of pulmonary nodule size on CT using film and computer display methods. Acad Radiol 2005; 12: 948–956.

[60] Marten K, Engelke C. Computer-aided detection and automated CT volumetry of pulmonary nodules. Eur Radiol 2007; 17: 888–901.

[61] Marten K, Auer F, Schmidt S, Rummeny EJ, Engelke C. Automated CT volumetry of pulmonary metastases: the effect of a reduced growth threshold and target lesion number on the reliability of therapy response assessment using RECIST criteria. Eur Radiol 2007; 17: 2561–2571.

[62] Vogel MN, Schmucker S, Maksimovic O, Hartmann J, Claussen CD, Horger M. Reduction in growth threshold for pulmonary metastases: an opportunity for volumetry and its impact on treatment decisions. Br J Radiol 2012; 85: 959–964.

[63] Wang J, Wu N, Cham MD, Song Y. Tumor response in patients with advanced non-small cell lung cancer: perfusion CT evaluation of chemotherapy and radiation therapy. AJR Am J Roentgenol 2009; 193: 1090–1096.

[64] Harvey C, Morgan J, Blomley M, Dooher A, de Souza N, Dawson P. Tumor responses to radiation therapy: use of dynamic contrast material-enhanced CT to monitor functional and anatomical indices. Acad Radiol 2002; 9(Suppl 1): S215–S219.

[65] Ng QS, Goh V, Carnell D, et al. Tumor antivascular effects of radiotherapy combined with combretastatin a4 phosphate in human non-small-cell lung cancer. Int J Radiat Oncol Biol Phys 2007; 67: 1375–1380.

[66] Ng QS, Goh V, Milner J, Padhani AR, Saunders MI, Hoskin PJ. Acute tumor vascular effects following fractionated radiotherapy in human lung cancer: In vivo whole tumor assessment using volumetric perfusion computed tomography. Int J Radiat Oncol Biol Phys 2007; 67: 417–424.

[67] Yabuuchi H, Hatakenaka M, Takayama K, et al. Non-small cell lung cancer: detection of early response to chemotherapy by using contrast-enhanced dynamic and diffusion-weighted MR imaging. Radiology 2011; 261: 598–604.

[68] Hegenscheid K, Behrendt N, Rosenberg C, et al. Assessing early vascular changes and treatment response after laser-induced thermotherapy of pulmonary metastases with perfusion CT: initial experience. AJR Am J Roentgenol 2010; 194: 1116–1123.

[69] Ma SH, Le HB, Jia BH, et al. Peripheral pulmonary nodules: relationship between multi-slice spiral CT perfusion imaging and tumor angiogenesis and VEGF expression. BMC Cancer 2008; 8: 186.

[70] Ng QS, Goh V, Fichte H, et al. Lung cancer perfusion at multidetector row CT: reproducibility of whole tumor quantitative measurements. Radiology 2006; 239: 547–553.

[71] Henzler T, Schmid-Bindert G, Schoenberg SO, Fink C. Diffusion and perfusion MRI of the lung and mediastinum. Eur J Radiol 2010; 76: 329–336.

[72] Ohno Y, Koyama H, Yoshikawa T, et al. Diffusion-weighted MRI versus ^{18}F-FDG PET/CT: performance as predictors of tumor treatment response and patient survival in patients with non-small cell lung cancer receiving chemoradiotherapy. AJR Am J Roentgenol 2012; 198: 75–82.

[73] Okuma T, Matsuoka T, Yamamoto A, Hamamoto S, Nakamura K, Inoue Y. Assessment of early treatment response after CT-guided radiofrequency ablation of unresectable lung tumours by diffusion-weighted MRI: a pilot study. Br J Radiol 2009; 82: 989–994.

[74] Chang Q, Wu N, Ouyang H, Huang Y. Diffusion-weighted magnetic resonance imaging of lung cancer at 3.0 T: a preliminary study on monitoring diffusion changes during chemoradiation therapy. Clin Imaging 2012; 36: 98–103.

[75] Choi NC, Fischman AJ, Niemierko A, et al. Dose-response relationship between probability of pathologic tumor control and glucose metabolic rate measured with FDG PET after preoperative chemoradiotherapy in locally advanced non-small-cell lung cancer. Int J Radiat Oncol Biol Phys 2002; 54: 1024–1035.

[76] Pottgen C, Levegrun S, Theegarten D, et al. Value of ^{18}F-fluoro-2-deoxy-D-glucose-positron emission tomography/computed tomography in non-small-cell lung cancer for prediction of pathologic response and times to relapse after neoadjuvant chemoradiotherapy. Clin Cancer Res 2006; 12: 97–106.

[77] Lee DH, Kim SK, Lee HY, et al. Early prediction of response to first-line therapy using integrated ^{18}F-FDG PET/CT for patients with advanced/metastatic non-small cell lung cancer. J Thorac Oncol 2009; 4: 816–821.

[78] Mac Manus MP, Hicks RJ, Matthews JP, et al. Positron emission tomography is superior to computed tomography scanning for response-assessment after radical radiotherapy or chemoradiotherapy in patients with non-small-cell lung cancer. J Clin Oncol 2003; 21: 1285–1292.

[79] de Geus-Oei LF, van der Heijden HF, Visser EP, et al. Chemotherapy response evaluation with ^{18}F-FDG PET in patients with non-small cell lung cancer. J Nucl Med 2007; 48: 1592–1598.